Design of OFDM Sequences for Joint Communications and Positioning Based on the Asymptotic Expected CRB

Arash Shahmansoori, Rafael Montalban, José A. López-Salcedo and Gonzalo Seco-Granados
Universitat Autònoma de Barcelona,
Bellaterra, Barcelona 08193, Spain
{arash.shahmansoori, rafael.montalban, jose.salcedo, gonzalo.seco}@uab.cat

Abstract—A key aspect to design an OFDM system for combined positioning and high-data-rate communications is to find optimal data and pilot power allocations. Previously, A capacity maximizing design by taking into account the effects of channel and time-delay estimation for finite number of subcarriers and channel taps has been investigated. Increasing the number of subcarriers and channel taps make the matrix inversions in the non-asymptotic bounds close to singular or badly conditioned. Furthermore, computational complexity of such a system designed by non-asymptotic bounds grows significantly. In this paper, a method based on the asymptotic expected Cramér-Rao bound of joint time-delay and channel coefficients by increasing the number of subcarriers and channel taps has been proposed. The method reduces the complexity of the design considerably. Specifically, by increasing the number of channel taps the number of operations to compute matrix inversions is significantly reduced by asymptotic bounds. Numerical results show that as the number of subcarriers increases, the asymptotic bounds converge to the non-asymptotic bounds. Moreover, even for a finite number of subcarriers or channel taps the difference between joint data and pilot power allocations is negligible compared to the non-asymptotic expected Cramér-Rao bounds.

Index Terms—OFDM, channel and time-delay estimation, asymptotic expected CRB, power allocation.

I. INTRODUCTION

The design of combined positioning and communications systems that can perform well in terms of high-data-rate transmission and delay estimation accuracy is a challenging problem. In general, the signals used for one application perform poorly in the other case. To design a signal which can be applied for both purposes, one needs to consider the system specifications for time-delay estimation accuracy and data-rate communications.

To date, different approaches have been adopted to design pilot symbols that improve the performance of channel estimators

[1]–[3]. The results show that equi-spaced, equi-powered pilots are optimal in terms of mean squared error. Pilot designs based on carrier frequency offset (CFO) estimation [4], or joint channel and CFO estimation [5] are considered by others. However, pilot design based on time delay estimation has received little attention. A pilot design based on joint CRB of channel and time delay is proposed in [6]. However, since CRBs in [6] are functions of specific channel realizations, the resulting pilots cannot be guaranteed to be optimal for all instances of random channels. The problem has been solved by designing based on averaging the CRB over a set of channel realizations known as Expected CRB (ECRB) [7]. In [7], joint design data and pilot power allocations for the case of limited number of subcarriers N and channel taps L is investigated. However, increasing the number of subcarriers and channel taps leads to very complex and close to singular matrix inversions using non-asymptotic bounds. Specifically, applying matrix inversion algorithms such as Gaussian elimination requires the computational complexity of the order $O(L^3)$ [8] for long channels which makes the proposed bounds in [7] complex and close to singular. A method based on the effect of increasing the number of subcarriers N and channel taps L on joint channel coefficients and clock offset estimation is proposed in [9]. However, the bounds are limited to a specific type of channel.

In this paper, we consider the effect of increasing the number of subcarriers N and channel taps L on the joint expected Cramér-Rao bound of time-delay and channel coefficients. First we analyze the problem of finding Asymptotic expected CRB by assuming large number of subcarriers. Also, we investigate the effect of increasing the number of channel taps L, which is usual in wire-line applications (e.g., VDSL and PLT), such that the ratio between the number of channel taps and subcarriers L/N is sufficiently small. Increasing the number of subcarriers and channel taps leads to very complex and close to singular matrix inversions using non-asymptotic bounds. Here, we aim to reduce the complexity to $O(L)$ by doing the inversion only at strong pilots and setting the rest of eigenvalues and their corresponding eigenvectors

to zero. Finally, we compare joint design of data and pilot allocations based on asymptotic bounds with non-asymptotic bounds using several numerical examples. Our results show that the difference for joint design of data and pilot allocations based on asymptotic bounds is negligible.

II. SYSTEM MODEL AND PRELIMINARIES

In this section, first we present a model of the OFDM system, then we propose the ECRB of the joint timing offset and channel coefficients estimation as a performance metric.

A. OFDM Signal Model

Using the same notation as [9], the continuous-time received signal from a standard OFDM symbol passed through a frequency selective channel, after removing the guard interval, is

$$y_N^{(a)}(t) = \sum_{k \in \mathbb{Z}} d_{N,k} g^{(a)}(t - kT) + v^{(a)}(t), \qquad (1)$$

where T is the sampling period at the transmitter such that $T_0 = NT$ is the observation window, N is the total number of subcarriers, $d_{N,k}$ represents the output from the inverse FFT (IFFT) block at the transmitter, and $v^{(a)}(t)$ is additive zero-mean complex Gaussian noise. Unlike [9], but without loss of generality, we assume that the impulse response $g^{(a)}(t)$ is a delta function with the time limit of $[0, LT)$ where L is the number of channel taps

$$g^{(a)}(t) = \sum_{l=0}^{L-1} h_l \delta(t - lT - \tau), \qquad (2)$$

where h_l is the channel coefficient of lth path and τ is the timing offset or equivalently the time delay of first path. Assuming the transmitter's and receiver's clocks are synchronized, the discrete-time received signal $y_N[n] = y_N^{(a)}(nT)$ is

$$y_N[n] = \frac{1}{\sqrt{N}} \sum_{n'=0}^{N-1} \sum_{l=0}^{L-1} D_{N,n'} h_l e^{j\frac{2\pi}{N} n'(n-l-\tau_d)} + v[n], \quad (3)$$

where $D_{N,n'}$ represents pilot subcarrier at the n'th frequency, and $\tau = \tau_d T$. In vector form we have

$$\boldsymbol{y}_N = \boldsymbol{R}_N(\tau_d)\boldsymbol{h} + \boldsymbol{v}_N, \qquad (4)$$

where

$$\boldsymbol{y}_N = [y_N[0], \dots, y_N[N-1]]^T,$$

$$\boldsymbol{v}_N = [v_N[0], \dots, v_N[N-1]]^T,$$

$$\boldsymbol{h} = [h_0, \dots, h_{L-1}]^T,$$

and the (n, l) element of $\boldsymbol{R}_N(\tau_d)$ is

$$[\boldsymbol{R}_N(\tau_d)]_{n,l} = \frac{1}{\sqrt{N}} \sum_{n'=0}^{N-1} D_{N,n'} e^{j\frac{2\pi}{N} n'(n-l-\tau_d)}.$$

Finally, taking the FFT of the output, we find

$$\boldsymbol{Y}_N = \boldsymbol{F}_{N,N}\boldsymbol{y}_N = \boldsymbol{F}_{N,N}\boldsymbol{R}_N(\tau_d)\boldsymbol{h} + \boldsymbol{V}_N, \qquad (5)$$

which describes the output of the OFDM system at the training phase. Also, one can obtain a similar model as in [6] by taking the DFT of (3) and writing the result in a vector notation as

$$\boldsymbol{Y}_N = \boldsymbol{D}_N \boldsymbol{\Gamma}(\tau_d) \boldsymbol{F}_{N,L} \boldsymbol{h} + \boldsymbol{V}_N, \qquad (6)$$

where $\boldsymbol{D}_N$ represents an $N \times N$ diagonal matrix of the input with the kth diagonal element $D_{N,k}$ representing the input at the kth subcarrier, $\boldsymbol{\Gamma}$ is an $N \times N$ diagonal matrix with the kth diagonal element $\exp(-j2\frac{\pi}{T}k\tau_d)$, and $\boldsymbol{F}_{N,L}$ contains the first L columns of a Discrete Fourier Transform (DFT) matrix. Note that the difference between our problem and the problems presented in [5], [9] is that here the timing offset is only multiplied by n', while in [9], sampling clock frequency offset is multiplied by both n' and n. Also, the problem differs from the case when frequency offset occurs [5] since in that case frequency offset is multiplied by n not n'.

B. Expected Cramér-Rao Bound

In this section, we present a closed-form expression for the expected CRB for the channel coefficients $\boldsymbol{h}$ and the timing offset τ_d. Note that the related results can be found in [5]–[7], [9]. Defining the parameter vector by $\boldsymbol{\theta} = [\boldsymbol{h}_R^T, \boldsymbol{h}_I^T, \tau_d]^T$, the corresponding Fisher information matrix (FIM) can be written as

$$\boldsymbol{J}_F = \frac{2}{\sigma^2} \Re \left[\frac{\partial \boldsymbol{\mu}^H}{\partial \boldsymbol{\theta}} \frac{\partial \boldsymbol{\mu}}{\partial \boldsymbol{\theta}^T} \right], \qquad (7)$$

where $\boldsymbol{\mu} = \boldsymbol{F}_{N,N}\boldsymbol{R}_N(\tau_d)\boldsymbol{h}$. One can easily find the FIM

$$\boldsymbol{J}_F = \frac{2}{\sigma^2} \begin{bmatrix} N\Re[\boldsymbol{U}_N] & -N\Im[\boldsymbol{U}_N] & N^2\Re[\boldsymbol{V}_N\boldsymbol{h}] \\ N\Im[\boldsymbol{U}_N] & N\Re[\boldsymbol{U}_N] & N^2\Im[\boldsymbol{V}_N\boldsymbol{h}] \\ N^2\Re[\boldsymbol{h}^H\boldsymbol{V}_N^H] & -N^2\Im[\boldsymbol{h}^H\boldsymbol{V}_N^H] & N^3\boldsymbol{h}^H\boldsymbol{W}_N\boldsymbol{h} \end{bmatrix},$$
$$(8)$$

where

$$\boldsymbol{U}_N = \frac{1}{N}\boldsymbol{R}_N^H(\tau_d)\boldsymbol{R}_N(\tau_d), \qquad (9)$$

$$\boldsymbol{V}_N = \frac{1}{N^2}\boldsymbol{R}_N^H(\tau_d)\boldsymbol{Q}_N(\tau_d), \qquad (10)$$

$$\boldsymbol{W}_N = \frac{1}{N^3}\boldsymbol{Q}_N^H(\tau_d)\boldsymbol{Q}_N(\tau_d), \qquad (11)$$

being $\boldsymbol{Q}_N(\tau_d) = d\boldsymbol{R}_N(\tau_d)/d\tau_d$. Using the well known block inversion matrix lemma [10] and defining a new estimation parameter $\tilde{\boldsymbol{\theta}} = [\boldsymbol{h}^T, \tau_d]^T$, we find

$$\mathbb{E}\left[||\hat{\boldsymbol{h}}_N - \boldsymbol{h}||^2\right] \geq \frac{\sigma^2}{2N}\left(2\text{tr}(\boldsymbol{U}_N^{-1}) + \gamma_N^{-1}||\boldsymbol{\beta}_N||^2\right), \quad (12)$$

$$\mathbb{E}\left[(\hat{\tau}_d^N - \tau_d)^2\right] \geq \frac{\sigma^2}{2N^3\gamma_N}, \qquad (13)$$

where

$$\boldsymbol{\beta}_N = \boldsymbol{U}_N^{-1}\boldsymbol{V}_N\boldsymbol{h}, \qquad (14)$$

$$\gamma_N = \boldsymbol{h}^H(\boldsymbol{W}_N - \boldsymbol{V}_N^H\boldsymbol{U}_N^{-1}\boldsymbol{V}_N)\boldsymbol{h}. \qquad (15)$$

Finally, taking the expectation with respect to channel coefficients and using Jensen's inequality, the approximate expression for the ECRB of the timing offset and the channel coefficients would be

$$\text{ECRB}_h \approx \frac{\sigma^2}{2N} \left(2\text{tr}(\boldsymbol{U}_N^{-1}) + \overline{\gamma}_N^{-1}||\overline{\boldsymbol{\beta}}_N||^2 \right), \quad (16)$$

$$\text{ECRB}_{\tau_d} \approx \frac{\sigma^2}{2N^3\overline{\gamma}_N}, \quad (17)$$

where

$$||\overline{\boldsymbol{\beta}}_N||^2 = \text{tr}\left((\boldsymbol{V}_N^H \boldsymbol{U}_N^{-H} \boldsymbol{U}_N^{-1} \boldsymbol{V}_N) \boldsymbol{R}_h \right), \quad (18)$$

$$\overline{\gamma}_N = \text{tr}\left((\boldsymbol{W}_N - \boldsymbol{V}_N^H \boldsymbol{U}_N^{-1} \boldsymbol{V}_N) \boldsymbol{R}_h \right), \quad (19)$$

where $\boldsymbol{R}_h$ is the channel covariance matrix. Note that the actual expected CRB is tighter than the above expressions due to Jensen's inequality. In the next section, we obtain the asymptotic ECRB for channel coefficients and timing offset where the number of subcarriers N is assumed to be sufficiently large.

III. ASYMPTOTIC EXPECTED CRAMÉR-RAO BOUND

In this section, we obtain an asymptotic expression for $\boldsymbol{U}_N$, and using a similar procedure as in [9], we conclude the expressions for $\boldsymbol{V}_N$ and $\boldsymbol{W}_N$. Unlike the expressions proposed in [9], we express the asymptotic values of $\boldsymbol{U}_N$, $\boldsymbol{V}_N$, and $\boldsymbol{W}_N$ in discrete frequency as a function of pilot powers since the final goal would be to design a system with optimal power allocation for joint communication and navigation.

A. Asymptotic Behavior for Finite Channels

Staring from the expression of $\boldsymbol{U}_N$ presented in (9), the (p,q) element of $\boldsymbol{U}_N$ is

$$[\boldsymbol{U}_N]_{p,q} =$$
$$\frac{1}{N} \sum_{l_1,l_2=0}^{N-1} D_{N,l_1}^* D_{N,l_2} e^{j\frac{2\pi}{N}(l_1-l_2)\tau_d} [\boldsymbol{M}^H(l_1)\boldsymbol{M}(l_2)]_{p,q}, \quad (20)$$

where

$$[\boldsymbol{M}^H(l_1)\boldsymbol{M}(l_2)]_{p,q} = e^{-j\frac{2\pi}{N}(ql_2-pl_1)} \psi_N^{(0)}((l_1-l_2)), \quad (21)$$

being

$$\psi_N^{(0)}((l_1-l_2)) = \frac{1}{N}\sum_{n=0}^{N-1} e^{-j\frac{2\pi}{N}n(l_1-l_2)}. \quad (22)$$

Replacing (21) and (22) in (20) and using the lemma proposed in [9] with $r = q - p + \tau_d$, $\alpha = 1/2$ and $\phi_N(k) = e^{-j\frac{2\pi}{N}pk}\psi_N^{(0)}(k)$, one can conclude that the terms for $l_1 \neq l_2$ in (20) almost surely converge to zero. Therefore, we obtain

$$[\boldsymbol{U}]_{p,q} = [\boldsymbol{U}_{N\to\infty}]_{p,q} = \frac{1}{N}\sum_{l=0}^{N-1} |D_{N,l}|^2 e^{-j\frac{2\pi}{N}(q-p)l}. \quad (23)$$

Similarly, the asymptotic expressions for $\boldsymbol{V}_N$ and $\boldsymbol{W}_N$ can be found as

$$[\boldsymbol{V}]_{p,q} = [\boldsymbol{V}_{N\to\infty}]_{p,q} = \frac{j\pi}{N}\sum_{l=0}^{N-1}\frac{l}{N}|D_{N,l}|^2 e^{-j\frac{2\pi}{N}(q-p)l}, \quad (24)$$

and

$$[\boldsymbol{W}]_{p,q} = [\boldsymbol{W}_{N\to\infty}]_{p,q} = \frac{4\pi^2}{3N}\sum_{l=0}^{N-1}(\frac{l}{N})^2|D_{N,l}|^2 e^{-j\frac{2\pi}{N}(q-p)l}. \quad (25)$$

In the following, we find a more compact form for the asymptotic expressions of channel coefficients and time delay and also we consider the case when the number of channel taps L is sufficiently large such that $L/N \to 0$. Replacing $|D_{N,l}|^2$ by P_l as the pilot power at the lth subcarrier, and using (23), (24), and (25) we obtain

$$\boldsymbol{U} = \boldsymbol{U}_{N\to\infty} = \frac{1}{N}\sum_{l=0}^{N-1} P_l \boldsymbol{e}(l)\boldsymbol{e}^H(l), \quad (26)$$

$$\boldsymbol{V} = \boldsymbol{V}_{N\to\infty} = \frac{j\pi}{N}\sum_{l=0}^{N-1}\frac{l}{N} P_l \boldsymbol{e}(l)\boldsymbol{e}^H(l), \quad (27)$$

$$\boldsymbol{W} = \boldsymbol{W}_{N\to\infty} = \frac{4\pi^2}{3N}\sum_{l=0}^{N-1}(\frac{l}{N})^2 P_l \boldsymbol{e}(l)\boldsymbol{e}^H(l), \quad (28)$$

where

$$\boldsymbol{e}(l) = [e^{j\frac{2\pi}{N}l(0)}, \dots, e^{j\frac{2\pi}{N}l(L-1)}]^T. \quad (29)$$

Note that (26), (27), and (28) can be interpreted as the sum of N, $L \times L$ matrices with the eigenvalues P_l and eigenvectors $\boldsymbol{e}(l)$ for $l = 0, \dots, N-1$. In matrix form, we have

$$\boldsymbol{U} = \boldsymbol{F}_{L,N}\boldsymbol{P}\boldsymbol{F}_{L,N}^H, \quad (30)$$

$$\boldsymbol{V} = j\pi\boldsymbol{F}_{L,N}\boldsymbol{f}\boldsymbol{P}\boldsymbol{F}_{L,N}^H, \quad (31)$$

$$\boldsymbol{W} = \frac{4\pi^2}{3}\boldsymbol{F}_{L,N}\boldsymbol{f}^2\boldsymbol{P}\boldsymbol{F}_{L,N}^H, \quad (32)$$

where $\boldsymbol{F}_{L,N}$ is the first L rows of the discrete Fourier transform matrix, and $\boldsymbol{P}$ and $\boldsymbol{f}$ are pilot power and derivative matrices respectively, defined as,

$$\boldsymbol{P} = \text{diag}\{P_0, \dots, P_{N-1}\}, \quad (33)$$

$$\boldsymbol{f} = \text{diag}\{\frac{0}{N}, \dots, \frac{N-1}{N}\}. \quad (34)$$

Consequently, asymptotic ECRB of channel coefficients and time delay can be found by replacing (30), (31), and (32) in (16) and (17),

$$N\text{ECRB}_h^{as} \approx \frac{\sigma^2}{2}\left(2\text{tr}(\boldsymbol{U}^{-1}) + \overline{\gamma}^{-1}||\overline{\boldsymbol{\beta}}||^2 \right), \quad (35)$$

$$N^3\text{ECRB}_{\tau_d}^{as} \approx \frac{\sigma^2}{2\overline{\gamma}}, \quad (36)$$

where

$$||\overline{\boldsymbol{\beta}}||^2 = \text{tr}\left((\boldsymbol{V}^H\boldsymbol{U}^{-H}\boldsymbol{U}^{-1}\boldsymbol{V})\boldsymbol{R}_h \right), \quad (37)$$

and

$$\overline{\gamma} = \text{tr}\left((\boldsymbol{W} - \boldsymbol{V}^H\boldsymbol{U}^{-1}\boldsymbol{V})\boldsymbol{R}_h \right). \quad (38)$$

B. Asymptotic Behavior for Long Channels

Finally, we analyze a special case where the number of channel taps L is sufficiently large such that $L/N \to 0$. In this case the Fisher information matrix (FIM) is close to singular or badly conditioned. For this type of problem, it is proved in [11] that instead of using the inverse of the FIM, we should apply the pseudo-inverse. This means that the inverse terms in (35) and (36), i.e. U^{-1} and U^{-2}, should be replaced by their pseudo-inverse $U^\dagger$ and $U^\dagger U^\dagger$ respectively. Using the eigenvalue decomposition, we have

$$U^\dagger = E^H \Sigma_1^{-1} E, \tag{39}$$

$$V = E^H \Sigma_2 E, \tag{40}$$

$$W = E^H \Sigma_3 E, \tag{41}$$

where E are normalized eigenvectors while the eigenvalues are stored in diagonal matrices Σ_1, Σ_2 and Σ_3. Note that by definition the pseudo-inverse of a matrix $U^\dagger$ is the inverse of its nonzero eigenvalues stored in diagonal matrix Σ_1 with the rest of entries are set to zero. Next, setting the eigenvectors corresponding to weak and zero eigenvalues to zero, we obtain $\widetilde{U}^\dagger = \widetilde{E}^H \widetilde{\Sigma}_1^{-1} \widetilde{E}$, $\widetilde{V} = \widetilde{E}^H \widetilde{\Sigma}_2 \widetilde{E}$, $\widetilde{W} = \widetilde{E}^H \widetilde{\Sigma}_3 \widetilde{E}$, where for sufficiently long channels we have $\widetilde{E}^H \widetilde{E} \approx I$, since $\widetilde{E}^H \widetilde{E} \approx \sum_{i=0}^{N_p-1} \alpha_{k_i} \alpha_{k_i}^H$ where α_{k_i} is the ith corresponding column of $\widetilde{E}^H$ to the eigenvalues greater than a threshold ζ that leads to identity since N_p converges to L by increasing L for a given threshold ζ (The larger L the smaller the threshold ζ). Replacing $\widetilde{U}$, $\widetilde{V}$, $\widetilde{W}$ in (37) and (38) and the result to (35) and (36), we find

$$N\overline{\text{ECRB}}_h^{as} \approx \frac{\sigma^2}{2} \left(2\text{tr}(\widetilde{\Sigma}_1^{-1}) + \overline{\gamma}_{L\gg1}^{-1} ||\overline{\beta}_{L\gg1}||^2 \right), \tag{42}$$

$$N^3 \overline{\text{ECRB}}_{\tau_d}^{as} \approx \frac{\sigma^2}{2\overline{\gamma}_{L\gg1}}, \tag{43}$$

where

$$||\overline{\beta}_{L\gg1}||^2 = \text{tr}\left(\widetilde{\Sigma}_2^2 \widetilde{\Sigma}_1^{-2} \widetilde{E} R_h \widetilde{E}^H \right), \tag{44}$$

$$\overline{\gamma}_{L\gg1} = \text{tr}\left(\left[\widetilde{\Sigma}_3 - \widetilde{\Sigma}_2^2 \widetilde{\Sigma}_1^{-1} \right] \widetilde{E} R_h \widetilde{E}^H \right). \tag{45}$$

Note that the ratio between $||\overline{\beta}_{L\gg1}||^2$ and $\overline{\gamma}_{L\gg1}$ can be written as

$$\overline{\gamma}_{L\gg1}^{-1} ||\overline{\beta}_{L\gg1}||^2 = \frac{\sum_{k\in\mathcal{H}} \widetilde{\sigma}_2^2(k) \widetilde{\lambda}_k}{\sum_{k\in\mathcal{H}} [\widetilde{\sigma}_3(k)\widetilde{\sigma}_1(k) - \widetilde{\sigma}_1(k)\widetilde{\sigma}_2^2(k)] \widetilde{\lambda}_k}, \tag{46}$$

where $\mathcal{H}$ represents the set of subcarriers that the eigenvalues of $\widetilde{E} R_h \widetilde{E}^H$ are not zero, $\widetilde{\lambda}_k$ is the kth eigenvalue of $\widetilde{E} R_h \widetilde{E}^H$, and $\widetilde{\sigma}_1(k)$, $\widetilde{\sigma}_2(k)$, and $\widetilde{\sigma}_3(k)$ are kth diagonal entries of Σ_1, Σ_2, and Σ_3 respectively. It is of interest to note that $\overline{\text{ECRB}}^{as}$ depends on the channel covariance matrix R_h by the eigenvalues of $\widetilde{E} R_h \widetilde{E}^H$ which can be considered as channel frequency response. In other words, parts of the frequency region with strong channel frequency response are used for estimation.

IV. CHANNEL CAPACITY

In this section we present a pilot design for joint communication and navigation based on asymptotic expected CRB for two cases. First, a more general form when the number of channel taps can be any limited number is investigated. Second, we assume sufficiently large number of channel taps L such that the ratio between channel taps and the number of subcarriers goes to zero $L/N \to 0$. We can rewrite signal model (6) as

$$Y_N = H\dot{D}_N + V_N, \tag{47}$$

where $\dot{D}_N = [D_{N,0}, \ldots, D_{N,N-1}]^T$, $H = \text{diag}\{H(0), \ldots, H(N-1)\}$, $H(k) = \gamma_\tau(k)\bar{H}(k)$, $\gamma_\tau(k) = \exp(-j\frac{2\pi}{T_0}k\tau)$, $\bar{H}(k) = F_{k,L}h$, and $F_{k,L}$ is the kth row of $F_{N,L}$. Replacing H by $\hat{H} + \tilde{H}$ in (47) we obtain

$$y = \hat{H}\dot{D}_N + \tilde{H}\dot{D}_N + V_N, \tag{48}$$

where $\hat{H}$ and $\tilde{H}$ represent the estimated value and the error, with the kth diagonal elements $\hat{H}(k) = \gamma_{\hat{\tau}}(k)F_{k,L}\hat{h}$ and $\tilde{H}(k) = \gamma_{\tilde{\tau}}(k)F_{k,L}\tilde{h}$ respectively. It can be shown that the lower bound of the capacity C_{lb} is of the form of [12]

$$C_{lb} = \frac{1}{N} \mathbb{E}\left[\log_2 \det(I + P_d R_{y_e}^{-1} \hat{H}\hat{H}^H) \right], \tag{49}$$

where P_d is an $N \times N$ diagonal matrix with $p_{d,k}$ representing data power at kth subcarrier and

$$R_{y_e} = P_d \mathbb{E}\left[\tilde{H}\tilde{H}^H \right] + \sigma^2 I. \tag{50}$$

So, we obtain

$$\mathbb{E}\left[\tilde{H}\tilde{H}^H \right] = \text{diag}\left\{ F_{k,L} \mathbb{E}\{\tilde{h}\tilde{h}^H\} F_{k,L}^H \right\}_{k\in\mathcal{D}}, \tag{51}$$

where $\mathcal{D}$ represents the set of subcarriers used for data transmission. We replace the term $\mathbb{E}\{\tilde{h}\tilde{h}^H\}$ in (51) by the asymptotic expected CRB. Depending on the assumption on the number of channel taps, one can replace $\mathbb{E}\{\tilde{h}\tilde{h}^H\}$ using (35) and (38) in their matrix forms for the finite number of channel taps and for a sufficiently large number of channel taps such that $L/N \to 0$ respectively. Note that the operation $F_{k,L}\mathbb{E}\{\tilde{h}\tilde{h}^H\}F_{k,L}^H$ in (51) can be interpreted as interpolating the asymptotic ECRB of channel coefficients at the subcarriers used for data transmission.

V. POWER ALLOCATION OPTIMIZATION

In this section, we formulate the optimization problem used for pilot design for joint communication and positioning. To maximize the cost function which is the lower bound of capacity (49), one needs to solve the following optimization problem

$$\begin{cases} \max_{p,b} & C_{lb}(p,b) \\ \text{s.t.} & \text{ECRB}_{\tau_d}^{as}(p,b) \leq \epsilon \\ & 1^T p \leq P_t \\ & p_i \geq 0; \quad \forall i \\ & b_i^2 - b_i = 0; \quad \forall i \end{cases} \tag{52}$$
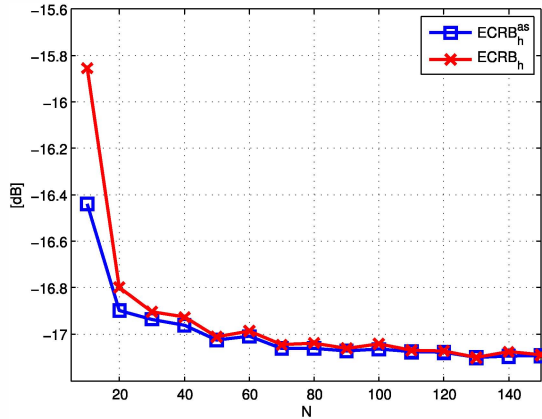
Fig. 1. Asymptotic behavior of ECRB_h^{as} versus number of subcarriers N.

TABLE I
RMSE OF THE DIFFERENCE BETWEEN ASYMPTOTIC AND
NON-ASYMPTOTIC ECRB OF TIME-DELAY

N	10	50	100	150
RMSE [dB]	-56.3961	-86.8914	-98.9957	-106.1279

where vector $\boldsymbol{p}$ is the power assigned to each of the subcarriers (i.e. $\boldsymbol{p} = \boldsymbol{p}_p + \boldsymbol{p}_d$), and $\boldsymbol{b}$ is a vector of length N with entries '1' in the positions of pilots and '0' in the positions of data. Consequently, we have ith element of pilots as $p_{p,i} = b_i p_i$ and ith element of data as $p_{d,i} = (1 - b_i)p_i$ with b_i defined as ith entry of vector $\boldsymbol{b}$. After solving optimization problem (52), the results show that only $L + 2$ elements of vector $\boldsymbol{b}$ are greater than zero and the rest of entries are close to zero meaning that just $L + 2$ subcarriers are used as pilots and the rest of subcarriers are set for data transmission.

VI. SIMULATION RESULTS

In this section we present the simulation results based on the asymptotic bounds. Within this section we use the number of subcarriers $N = 48$, total power for pilots and data $P_t = 5$, noise power $\sigma^2 = 0.01$, minimum accuracy in time-delay estimation is $\epsilon = 0.002$, diagonal channel covariance matrices of sizes 4×4 with $R_h = \text{diag}([1.8949; 1.6222; 1.4209; 1.9405])$, 6×6 with $R_h = \text{diag}([1.8949; 1.6222; 1.4209; 1.9405; 1.3209; 1.1405])$, and finally 8×8 with $R_h = \text{diag}([1.8949; 1.6222; 1.4209; 1.9405; 1.8949; 1.6222; 1.4209; 1.9405])$.

Fig. 1 shows the asymptotic behavior of the ECRB of channel coefficients ECRB_h^{as} comparing to the non-asymptotic bound ECRB_h by increasing the number of subcarriers N. The result shows that even for the finite number of subcarriers (e.g. for $N = 48$) the asymptotic bound converges to the non-asymptotic bound. The asymptotic behavior of the ECRB of time-delay $\text{ECRB}_{\tau_d}^{as}$ comparing to the non-asymptotic bound ECRB_{τ_d} is shown in Table I. This is to make the difference
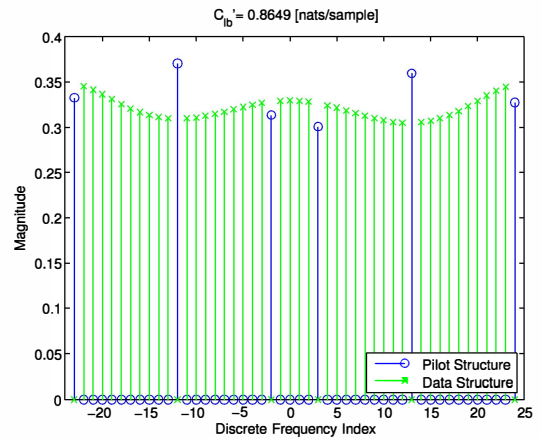
(a)
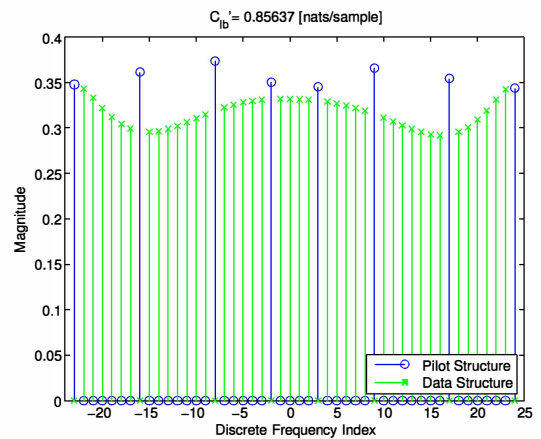
(b)
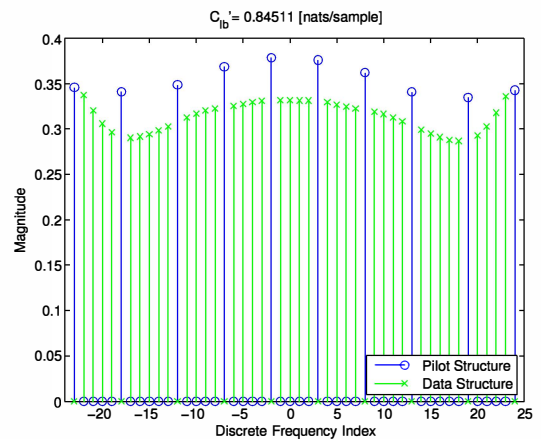
(c)

Fig. 2. Joint design of pilot and data power allocations using asymptotic ECRB for channels of length (a) $L = 4$, (b) $L = 6$, and (c) $L = 8$.

visible due to the fact that the convergence by increasing the number of subcarriers for $\text{ECRB}_{\tau_d}^{as}$ is of the order N^3 that is much faster than the convergence for ECRB_h^{as} that is of the order of N. The Root Mean Square Error (RMSE) between $\text{ECRB}_{\tau_d}^{as}$ and ECRB_{τ_d} is of the order of -56.4dB to

-106.13dB for N from 10 to 150 respectively.

Fig. 2 shows the joint design of pilots and data power allocations for IEEE 802.11 channel model with maximum number of paths $L = \lceil 10 \times \sigma_\tau / T_s \rceil$ where σ_τ is the RMS delay spread and T_s represents the sampling period. Fig. 2 shows the joint design of pilots and data power allocations based on the proposed channel model with maximum number of paths $L = 4$, $L = 6$, and $L = 8$, with diagonal channel covariance matrices, i.e. independent channel coefficients, defined in the simulation parameters, and number of subcarriers $N = 48$. The results show that using the channel of length L joint design of pilots and data power allocations requires $L + 2$ pilots for estimation with the rest of subcarriers saved for data transmission. Obviously, increasing the number of taps from $L = 4$ to $L = 8$ reduces the capacity by around 2.3% since the number of subcarriers for data transmission is reduced.

Fig. 3 studies the trade-off between capacity and time-delay estimation accuracy. The dashed-line curves with upward and downward triangle marks represent the capacity achieved by solving the optimization problem (52) without any restriction on the pilot distributions using non-asymptotic and asymptotic bounds respectively. For a given accuracy in the estimation of time-delay represented by ϵ the difference between capacity achieved by asymptotic and non-asymptotic bounds is negligible. However, using the asymptotic bounds simplify the joint design problem of data and pilot power allocations significantly specially by increasing the number of channel taps L.

The curves with square and circle marks represent maximum achievable capacity obtained by the solution to the problem (52) where subcarriers are allowed to be shared by pilot and data symbols for non-asymptotic and asymptotic bounds respectively. Note that by losing the time-delay accuracy ϵ down to 0.014 and higher arbitrary joint design problem based on asymptotic and non-asymptotic bounds converge to the same amount of capacity. We use the arbitrary designs of data and pilot power allocations as the upper bound of the maximum achievable capacity.

VII. CONCLUSION

Using asymptotic bounds one can reduce the computational complexity of the optimization problem specially by increasing the number of subcarriers N and channel taps L. In this paper, the performance of near-optimal pilot and data power allocations for the case of asymptotic bounds is compared with the traditional non-asymptotic bounds. Results show that after a certain number of subcarriers which can be as low as $N = 48$, asymptotic bounds converge to the non-asymptotic bounds. Further, the performance of joint data and pilot power allocations is only affected negligibly even for the limited number of subcarriers and channel taps.
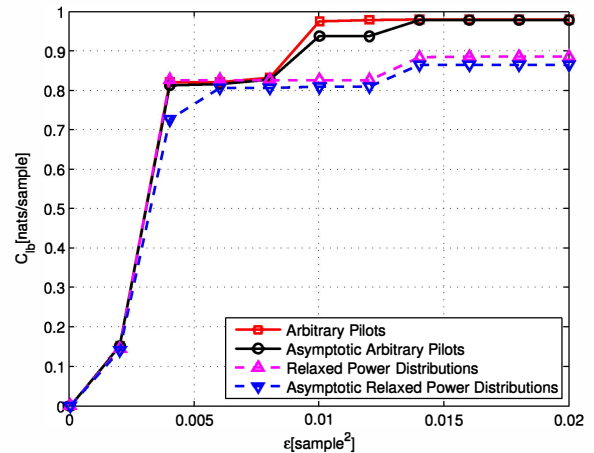
Fig. 3. Channel capacity versus desired value of time-delay estimation accuracy.

REFERENCES

[1] R. Negi and J. Cioffi, "Pilot tone selection for channel estimation in a mobile OFDM system," *IEEE Transactions on Consumer Electronics*, vol. 44, pp. 1122–1128, Aug. 1998.

[2] I. Barhumi, G. Leus, and M. Moonen, "Optimal training design for MIMO OFDM systems in mobile wireless channels," *IEEE Transactions on Signal Processing*, vol. 51, no. 6, pp. 1615–1624, Jun. 2003.

[3] H. Minn and N. Al-Dhahir, "Optimal training signals for MIMO-OFDM channel estimation," *IEEE Transactions on Wireless Communications*, vol. 5, no. 5, pp. 1158–1168, May. 2006.

[4] H. Minn and S. Xing, "An optimal training signal structure for frequency-offset estimation," *IEEE Transactions on Communications*, vol. 53, no. 2, pp. 343–355, Feb. 2005.

[5] P. Stoica and O. Besson, "Training sequence design for frequency offset and frequency-selective channel estimation," *IEEE Transactions on Communications*, vol. 51, no. 11, pp. 1910–1917, Nov. 2003.

[6] M.D. Larsen, G. Seco-Granados, and A.L. Swindlehurst, "Pilot optimization for time-delay and channel estimation in OFDM systems," in *IEEE International Conference on Acoustics, Speech and Signal Processing (ICASSP)*. 2011, pp. 3564–3567, IEEE.

[7] R. Montalban, J. A. Lopez-Salcedo, G. Seco-Granados, and A. L. Swindlehurst, "Power allocation method based on the channel statistics for combined positioning and communications OFDM systems," in *IEEE International Conference on Acoustics, Speech and Signal Processing (ICASSP)*. 2013, pp. 4384–4388, IEEE.

[8] S. Delič and Ž. Jurič, "Some improvements of the gaussian elimination method for solving simultaneous linear equations," in *IEEE International Convention on Information and Cummunication Technology Electronics and Microelectronics (MIPRO)*. 2013, pp. 96–101, IEEE.

[9] S. Gault, W. Hachem, and P. Ciblat, "Joint sampling clock offset and channel estimation for ofdm signals: Cramer-rao bound and algorithms," *IEEE Transactions on Signal Processing*, vol. 54, no. 5, pp. 1875–1885, May. 2006.

[10] S. M. Kay, *Fundamentals of Statistical Signal Processing: Estimation Theory*, Prentice Hall, New York, NY, USA, 2010.

[11] P. Stoica and T. Marzetta, "Parameter estimation problems with singular information matrices," *IEEE Transactions on Signal Processing*, vol. 49, no. 1, pp. 87–90, Jan. 2001.

[12] B. Hassibi and B. M. Hochwald, "How much training is needed in multiple-antenna wireless links," *IEEE Transactions on Information Theory*, vol. 49, no. 4, pp. 951–963, Apr. 2003.